This article has been accepted for publication in a future issue of this journal, but has not been fully edited. Content may change prior to final publication. Citation information: DOI 10.1109/JLT.2017.2781702, Journal of Lightwave Technology

Bidirectional red-light passively Q-switched all-fiber ring lasers with carbon nanotube saturbale absorber

Wensong Li, Chunhui Zhu, Xiaofeng Rong, Jiaji Wu, Huiying Xu, Fengqiu Wang, Zhengqian Luo, *Senior Member, IEEE*, and Zhiping Cai

***Abstract*—We report bidirectional red-light passively Q-switched all-fiber lasers based on a ring-cavity configuration using single-wall carbon nanotubes (SWNTs) as saturable absorber (SA). By manipulating the cavity design and intra-cavity polarization state, two sets of output pulses with different features could be achieved from the clockwise (C.W.) and counterclockwise (C.C.W.) directions, respectively. In the C.W. direction, the lasers generate the wavelength of 635.4 nm, the pulse trains with minimum pulse duration of 1.35 μs (1.51 μs) and the repetition rate ranging from 65.2 to 143 kHz (67.8 to 96.5 kHz). In the C.C.W. direction, the lasers, also emitting at 635.4 nm, deliver the pulse trains with minimum pulse duration of 0.81 μs (3.59 μs), as well as the repetition rate range of 57.5-98.2 kHz (37.2-58.9 kHz). This is, to the best of our knowledge, the first demonstration of bidirectional red-light passively Q-switched all-fiber ring lasers based on SWNT-SA.**

***Index Terms*—Fiber lasers, nanomaterials, saturable absorber, passive Q-switching, visible laser**

I. Introduction

SHORT-pulse all-fiber lasers have been of great interest for widespread industry and scientific research applications, due to its inherent compactness, simplicity and efficient heat dissipation [1]-[4]. Q-switching mechanism, which has been well known and intensively studied for decades, is mainly involved for short pulse generation with pulse duration of μs or ns level and low repetition rate of kHz. The dominant technology is based on a passively Q-switched scheme without resorting to complex and costly electrical modulators [5], which is enabled by a nonlinear element, i.e. saturable absorber (SA).

This work was partially supported by National Natural Science Foundation of China (11674269, 61275050), Science Funds for Distinguished Young Scientists of Fujian Province (2017J06016), Shenzhen Science and Technology Projects (JCYJ20160414160109018).

W. Li, X. Rong, J. Wu, H. Xu, Z. Luo, and Z. Cai are with the Department of Electronic Engineering, Xiamen University, Xiamen 361005, China (email: zpcai@xmu.edu.cn).

C. Zhu and F. Wang are with the School of Electronic and Engineering, Collaborative Innovation Center of Advanced Microstructures, Nanjing University, Nanjing 210023, China.

Currently, the commercial SAs are based on semiconductor quantum wells, known as semiconductor saturable absorber mirrors (SESAMs) [6], [7]. Limited operation bandwidth and high fabrication cost of SESAMs have stimulated the continuous motivations to find versatile SAs with ultra-broad operation bandwidth and the facile accessibility. Since 1990s, nanomaterial-based SAs, including single-wall carbon nanotubes (SWNTs) [8]-[11], graphene [12]-[16], transition-metal dichalcogenides (TMDs) [17]-[23], topological insulators (TIs) [24]-[30], black phosphorus (BP) [31]-[35], filled skutterudites (FSs) [36], and MXenes [37] have been demonstrated as effective SAs for pulsed fiber lasers at infrared wavelengths. Along with the rapid advances in infrared fiber lasers based on nanomaterials SAs, there is also continued interest in the development of fiber lasers at wavelengths extendable to the visible region. Herein, our recent reports demonstrated the visible pulsed fiber lasers using TMDs [38], [39], TIs [40], and BP [41]. As the first nanomaterial-based SA, SWNTs have been extensively explored in pulsed fiber lasers due to the advantages including subpicosecond recovery time, broadband tunability and compatible to fiber [42]-[44]. In SWNTs the tube diameter controls the bandgap, thus, defining the operating wavelength. Utilizing such a design guideline, SWNT-based pulsed fiber lasers have been demonstrated mainly across the near-infrared spectral range [45]-[49]. And recently, Xu et al. reported ultra-broadband saturable absorption properties of SWNTs using the combination of Z-scan and degenerate pump-probe techniques, and experimentally validated that nonlinear absorption of SWNTs could extend into the visible region [50]. Additionally, our successive work also reported a deep-red light short pulse generation from SWNT-based passively Q-switched all-fiber lasers [51]. The motivation that triggered this study was shorter-wavelength operation achievable from SWNT-based pulsed all-fiber lasers (e.g., at red, green or ultraviolet), which would further reveal that SWNTs could act as an ultra-broad bandwidth SA. Meanwhile, different from the unidirectional ring cavity design, the bidirectional cavity configuration enables the pulsed lasers to operate without isolators. The bidirectional pulsed lasers are very useful for gyroscopes [52], [53], synthesis of optical waveform [54], [55], sensors [56], [57], and other versatile applications.

In this work, we demonstrate SWNT-based bidirectional red-light passively Q-switched all-fiber lasers for the first time. By controlling the cavity design and intra-cavity polarization

This article has been accepted for publication in a future issue of this journal, but has not been fully edited. Content may change prior to final publication. Citation information: DOI 10.1109/JLT.2017.2781702, Journal of Lightwave Technology

state of light, bidirectional short pulse operation with distinct output features are readily realized from the same laser cavity. As a comparison, two types of bidirectional Q-switched all-fiber lasers based on 0.9-m-length and 1.4-m-length active fibers are proposed. Stable Q-switched operations achieved generate the output pulses with minimum pulse duration of 0.81-3.59 μs and the repetition rate of 37.2-143 kHz, for both the C.W. and C.C.W. directions. Such all-fiber ring lasers provide output pulses with selective characteristics that could find much more attractive applications.

II. Characterization of the SWNT-SA

In our experiments, the SWNT sample was commercially-available purified one that was prepared by the electric arc-discharge technique [50]. A SWNT/polyvinyl alcohol (PVA) film was fabricated by evaporating the SWNT polymer composite solution to dryness. For the practical use, the as-prepared SWNT/PVA film is cut into small pieces and sandwiched between two fiber connectors [38]. Fig. 1(a) shows the optical absorption curves of the SWNT/PVA film and pure PVA film, which were recorded by an UV/VIS spectrometer (Perkin Elmer, Lambda750). The absorbance of the SWNT/PVA film is 0.32 and 0.30 at two wavelengths of 635 nm and 700 nm, respectively. However, the corresponding value for the pure PVA film is estimated to be only 0.04.

Fig. 1(b) gives the nonlinear power-dependent absorbance measurement of the SWNT-SA at the visible wavelength of 700 nm. The blue circle represents the experimental result, which was measured by using Z-scan technique with a balanced twin-detector [58]. The laser source for the experimental setup is an optical parametric amplifier, which is pumped by a 1 kHz, 800 nm Ti: Sapphire amplifier system (Coherent Inc.), delivering ~100 fs pulses. The red line in Fig. 1(b) represents the fitted result, which was evaluated by using a classic saturable absorber model based on the following equation (1) [50], [59].

$$\alpha(I) = \frac{\alpha_0}{1 + I/I_{\mathrm{sat}}} + \alpha_{ns} \tag{1}$$

Where α denotes the linear absorption, α_0 is the saturable absorption, α_{ns} is the non-saturable absorption, so $\Delta T = \alpha_0/(\alpha_0 + \alpha_{ns})$ represents the modulation depth, I and I_{sat} are the laser radiation intensity and saturation intensity, respectively. As shown in Fig. 1(b), the saturable absorption α_0 and non-saturable absorption α_{ns} are 19% and 81%, respectively. The calculated modulation depth of ΔT = 19% is measured at the wavelength of 700 nm. The saturation intensity I_{sat} is about 400 MW/cm^2. These results confirm that the SWNT-SA could provide saturable absorption at visible 700 nm wavelength, promising for pulse generation in the visible region [51].

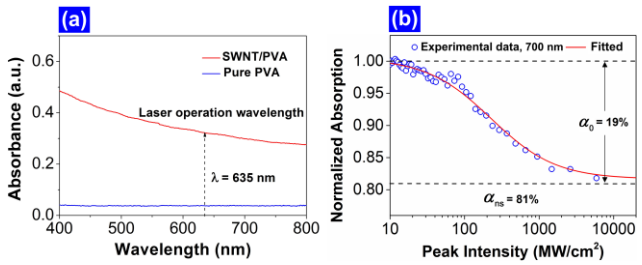

Fig. 1. (a) Linear absorption spectrum of the SWNT/PVA film in comparison with pure PVA film. The laser operation wavelength is shown as a dashed black line. (b) Nonlinear absorption characterization for 700 nm with saturable absorption fitting (red solid line).

III. Experimental Details

The schematic diagram and experimental photograph of the proposed bidirectional red passively Q-switched all-fiber lasers are shown in Fig. 2(a) and (b), respectively. The laser ring cavity consists of a wavelength division multiplexer (WDM), followed by Pr:ZBLAN fiber, polarization controller (PC), SWNT-SA, and optical coupler (OC). Here, the pump source is characterized by a house-made laser diode (LD) pigtail output based on the silicate single mode fiber (SMF) 630-HP (Nufern; core/cladding: 3.5/125 μm, NA: 0.13), which has a center wavelength of 444 nm and a maximum output power of ~ 0.4 W. A 0.9-m-length or 1.4-m-length Pr:ZBLAN fiber (Le Verre Fluoré; core/cladding: 6/125 μm, NA: 0.15, Pr^{3+}: 1000 ppm), with absorption coefficient of ~ 18.8 dB/m at 444 nm and intrinsic loss of less than 0.1 dB at 635 nm, is used as the gain medium. The Pr:ZBLAN fiber is pumped by the blue LD through a 630-HP fiber-based fused 444/630 nm WDM coupler. In the experiments, two ceramic sleeves with an inner diameter of 2.5 mm were utilized to realize the high-efficiency coupling between the Pr:ZBLAN fiber and the silicate SMF 1060-XP (Nufern; core/cladding: 5.8/125 μm, NA: 0.14). The PC is used to adjust the intracavity birefringence. The SWNT-based SA acts as a switcher to modulate the intracavity loss, which is assembled by sandwiching a free-standing SWNT-PVA film between two fiber ferrules that are self-made SMF 1060-XP pigtails. A 630-HP fiber-based 2×2 10/90 OC (Operating wavelength: 630 nm) extracts the ~10% signal from the clockwise (C.W.) and counter-clockwise (C.C.W.) directions for measurement. Without an imposed optical isolator inserted in the ring cavity, bidirectional operation is achieved reasonably. The total cavity lengths of the proposed two all-fiber ring lasers are 4.5 m and 5.0 m, respectively.

This article has been accepted for publication in a future issue of this journal, but has not been fully edited. Content may change prior to final publication. Citation information: DOI 10.1109/JLT.2017.2781702, Journal of Lightwave Technology

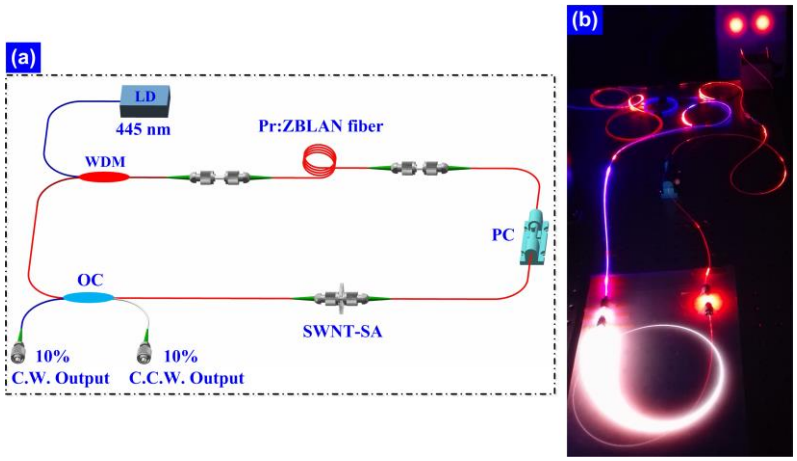

Fig. 2. (a) Schematic of the proposed all-fiber ring laser setup, where LD, WDM, PC and OC are laser diode, wavelength division multiplexer, polarization controller and output coupler, respectively. C.W.: clockwise, C.C.W.: counter-clockwise. (b) Experimental photograph of bidirectional red passively Q-switched all-fiber ring laser configuration.

The output powers are measured by two power meters (Ophir, Nova P/N 1Z02413 and Coherent, PM3). And the output spectra are recorded by two optical spectrum analyzers (Ocean Optics, HR4000/USB4000). The output Q-switched performance is monitored by two digital oscilloscopes with bandwidths of 100MHz (Tektronix TBS1102, 1 GS/s sampling rate) and 500 MHz (Tektronix TDS4054B, 2.5 GS/s sampling rate), together with two Si Biased detectors with rise time of 1 ns (Thorlabs, DET10A), followed by a radio-frequency (RF) spectrum analyzer (Gwinstek, GSP-930).

IV. Results and Comparisons

A. *Bidirectional Red CW Ring Laser*

The bidirectional red CW ring laser without a SWNT-SA was firstly produced. To confirm the CW operation, we investigated the laser output with an oscilloscope. No pulse trains were observed despite increasing the incident pump power and adjusting the polarization controller, as similar to our previous work [41]. Fig. 3 reports the output optical spectra of red CW ring lasers in both C.W. and C.C.W. directions. As shown in Fig. 3(a), we simultaneously recorded the lasing properties of the CW red ring laser with a 0.9-m-length active fiber, which presents a red-light wavelength of 635.7 nm at an incident-pump-power of 97.2 mW. In the inset of Fig. 3(a), a zoom-in image of the optical spectra for C.W. and C.C.W. directions is displayed. The output optical spectra of the CW red ring laser with a 1.4-m-length active fiber under an incident-pump-power of 91.8 mW were also measured. As plotted in Fig. 3(b) and its inset, a red-light wavelength of 635.7 nm is illustrated. But the wavelength profile has two peaks at 634.7 nm and 635.7 nm, respectively, which is due to a wide gain bandwidth (~3 nm) of red-light wavelength in the active fiber [38].

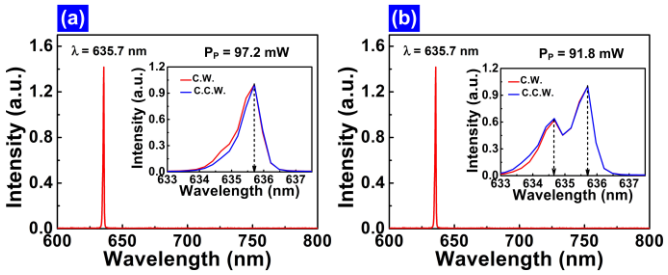

Fig. 3. Output optical spectra of red CW ring lasers with the active-fiber lengths of (a) 0.9 m and (b) 1.4 m, respectively. Insets: the close-up views of the optical spectra in both C.W. and C.C.W. directions.

Fig. 4 illustrates the output power characteristics of the red CW ring lasers. In the case of a 0.9-m-length active fiber based ring laser, the change of the output power with respect to the incident pump power is given in Fig. 4(a). The output powers of 2.9 mW and 2.2 mW at the incident-pump-power of 127.8 mW with the lasing threshold of ~50 mW, corresponding to C.W. and C.C.W. directions, respectively, were simultaneously measured. The slope efficiencies are estimated to be 3.8% and 2.9%, respectively. In comparison with those above parameters, the red CW ring laser with a 1.4-m-length active fiber has the output powers of 1.1 mW (C.W.) and 3.5 mW (C.C.W.) at the incident-pump-power of 127.8 mW, with a lasing threshold of ~55 mW as well as the slope efficiencies of 1.4% (C.W.) and 4.6% (C.C.W.). In order to protect the fiber ring cavity components, we did not further increase the incident-pump-power for enhancing the output-power. Here, the implementations towards the laser cavity design and intra-cavity polarization state of light are the reasons behind the different output powers [60], which stem from gain and loss in a distinct level for both directions. Due to the low output coupling value (10%), the proposed red ring lasers are characterized by low output power and low slope efficiency.

This article has been accepted for publication in a future issue of this journal, but has not been fully edited. Content may change prior to final publication. Citation information: DOI 10.1109/JLT.2017.2781702, Journal of Lightwave Technology

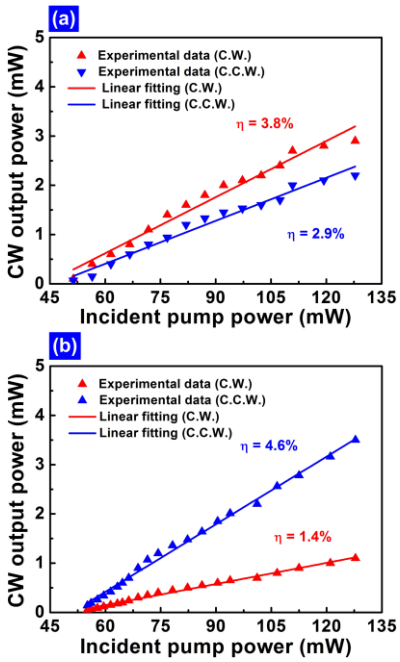

Fig. 4. Output power characteristics of bidirectional red CW ring lasers with (a) 0.9-m-length active fiber and (b) 1.4-m-length active fiber, respectively.

B. 0.9-m-length Active Fiber Based Bidirectional Red Q-switched ring laser

By integrating the SWNT-SA into the fiber ring cavity, the Q-switching state could be achieved. When increased the incident-pump-power to ~81 mW, the red CW ring laser came out. Obviously, this CW laser threshold with SWNT-SA is higher than the one (50 mW) without SWNT-SA. Thus, the insertion loss of the SWNT-SA is estimated to be 2.1 dB at 635 nm. When the incident-pump-power was increased to 83.6 mW, stable Q-switched outputs from the C.W. direction could be observed on the oscilloscope screen. However, until an incident-pump-power of 87.1 mW, the stable Q-switched operation from the C.C.W. direction could be achieved.

Fig. 5 shows the output oscilloscope traces of the red Q-switched ring laser in both C.W. and C.C.W. directions. The pulse-train evolution by increasing incident-pump-power is clearly exhibited. In C.W. direction, the number of the pulses captured increases from 13 pulses to 27 pulses over the same time period as the incident-pump-power is raised from 83.6 to 100.6 mW, corresponding to the repetition rate ranging from 65.2 to 137.7 kHz, as shown in Fig. 5(a). One can see from Fig. 5(b), in C.C.W. direction an increase of the incident-pump-power from 87.1 to 98.9 mW leads to the variation of the pulse trains from 57.5 to 83.3 kHz.

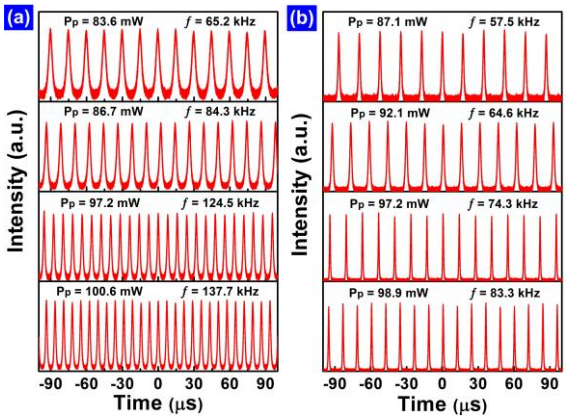

Fig. 5. The oscilloscope traces with respect to different incident pump powers for 0.9-m-length active fiber based bidirectional red Q-switched ring laser: (a) in C.W. direction, and (b) in C.C.W. direction.

Fig. 6 further gives the proposed red Q-switched ring laser characteristics for both directions. From Fig. 6(a), at an incident-pump-power of 97.2 mW, the single pulse shape presents a symmetric Gaussian-like intensity profile with pulse duration of 1.48 μs. It should be mentioned that the corresponding oscilloscope trace with a repetition rate of 124.5 kHz has been plotted in Fig. 5(a), which has a pulse-intensity fluctuation as low as 5%. In Fig. 6(b) is shown the RF spectrum. The signal-to-noise ratio (SNR) of the fundamental frequency peak at 124.5 kHz is recorded to be ~43 dB, comparable to those reported passively Q-switched red-light/near-infrared fiber lasers utilizing 2D materials as SAs [40], [41], [61]-[63], indicating a good stability of the red Q-switched outputs in the C.W. direction that is suitable for practical applications. Correspondingly, Fig. 6(c) also reports a symmetric Gaussian-like single pulse envelope, which has pulse duration of 0.87 μs at the incident-pump-power of 97.2 mW from the C.C.W. direction. As shown in Fig. 6(d), the RF SNR is about 40 dB at the fundamental frequency of 74.3 kHz, which is comparable to our previous works on visible Q-switched Fabry-Perot fiber lasers using 2D-material-based SAs [38], [40], [41]. Likewise, these results verify the good stability of the red Q-switched operation in the C.C.W. direction, indicating a promising capacity of this laser.

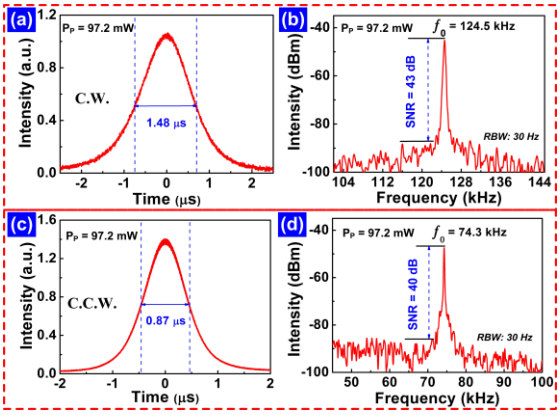

Fig. 6. Red Q-switched ring laser characteristics. (a) Single pulse shape and (b) RF output spectrum at the fundamental frequency of 124.5 kHz for the C.W. direction (upper). (c) Single pulse profile and (d) RF output spectrum at the fundamental frequency of 74.3 kHz for the C.C.W. direction (lower).

This article has been accepted for publication in a future issue of this journal, but has not been fully edited. Content may change prior to final publication. Citation information: DOI 10.1109/JLT.2017.2781702, Journal of Lightwave Technology

C. 1.4-m-length Active Fiber Based Bidirectional Red Q-switched Ring Laser

Firstly, under an incident-pump-power of ~85 mW, the red CW laser was running-up. The CW laser threshold with SWNT-SA is higher than the one (~55 mW) without SWNT-SA. Here, the insertion loss of the SWNT-SA is calculated to be 1.9 dB at 635 nm. Further increasing the incident-pump-power to 86.7 mW, stable Q-switched pulses was initiated in the C.C.W. direction, until 88.2 mW the stable Q-switching from the C.W. direction emerged.

Fig. 7 summarizes the output properties of the proposed red Q-switched ring laser at an incident-pump-power of 91.8 mW. In the case of C.W. direction, a SNR of ~42 dB at the fundamental frequency of 79.4 kHz was measured, followed by the corresponding oscilloscope trace with a pulse intensity-fluctuation of ~3% and its single pulse shape with pulse duration of 1.70 μs are separately recorded, as presented in sequence from Fig. 7(a) to Fig. 7(c). For the output pulses in C.C.W. direction, Fig. 7(d) gives the RF spectrum, showing a ~40 dB SNR at the fundamental frequency of 45.8 kHz. Fig. 7(e) shows the corresponding pulse trains, which has a less than 5% intensity-fluctuation. Then, the zoom-in image of this output pulse is also exhibited in Fig. 7(f), showing a symmetric Gaussian-like shape with pulse duration of 3.76 μs. These above results confirm that such a Q-switched laser is also suitable for practical applications.

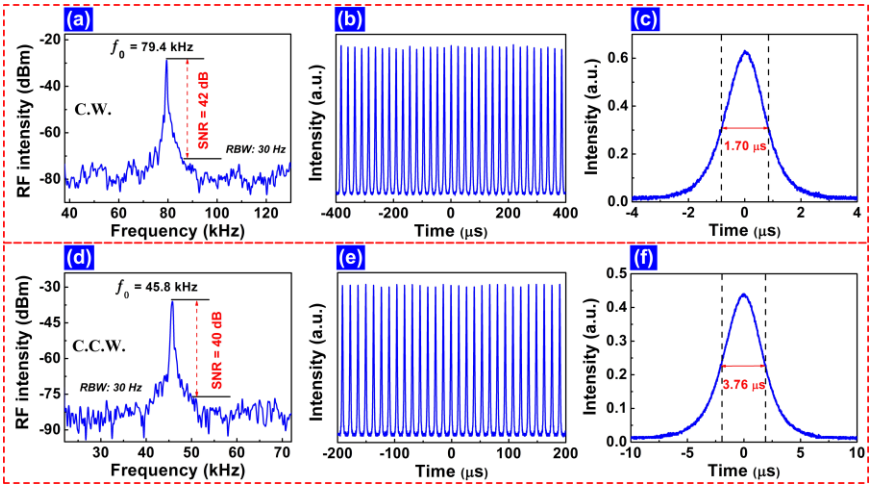

Fig. 7. Measured output properties of bidirectional red Q-switched ring laser based on 1.4-m-length active fiber in C.W. direction (upper) and C.C.W. direction (lower) at an incident-pump-power of 91.8 mW. (a, d) RF output spectra. (b, e) The oscilloscope traces. (c, f) The corresponding singe pulse shapes.

D. Experimental Comparisons and Discussions

Fig. 8(a) and (b) depict the optical spectra of both 0.9-m-length and 1.4-m-length active fiber based bidirectional red Q-switched ring lasers. Two sets of red Q-switched ring lasers have a similar lasing line 635.4 nm for the C.W. and C.C.W. directions at P_P = 97.2 mW and P_P = 91.8 mW, respectively. Whereas some minor differences exist in the lasing spectral profiles, as separately shown in the insets of Fig. 8(a) and (b). Such an appearance is mainly because the output pulses experience gain competition effects in the laser cavity (i.e., gain and loss in a different level) [53]. Fig. 8(c) and (d) show the variations of the average output power of the bidirectional red Q-switched ring lasers with respect to different incident pump powers. For the 0.9-m-length active fiber based Q-switched ring laser, one can see from Fig. 8(a), the average output power linearly increased with the incident pump power, generating the maximum values of 0.39 and 0.29 mW, respectively, corresponding to the C.W. and C.C.W. directions. As for the 1.4-m-length active fiber based one, Fig. 8(b) clearly shows the linear dependence of the average output power on the incident pump power. The recorded maximum average output powers are 0.046 and 0.33 mW, respectively, for the C.W. and C.C.W. directions. Obviously, these results are similar to the above-described CW situation.

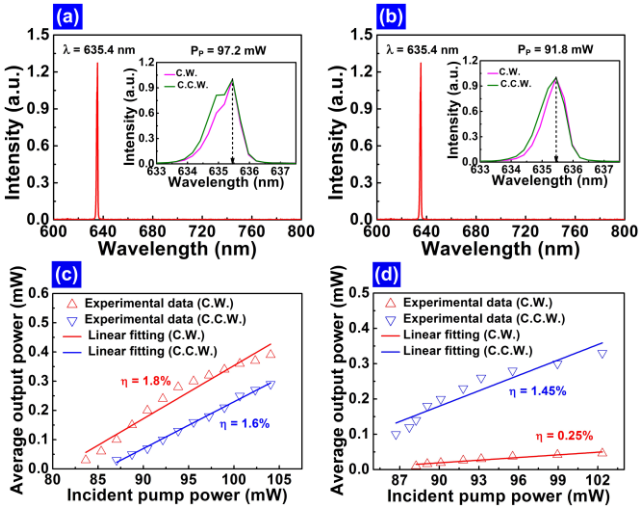

Fig. 8. Output characteristics of red Q-switched ring lasers based on (a, c) 0.9-m and (b, d) 1.4-m active-fiber lengths. Insets of (a) and (b): the close looks at 635.4 nm for both C.W. and C.C.W. directions.

This article has been accepted for publication in a future issue of this journal, but has not been fully edited. Content may change prior to final publication. Citation information: DOI 10.1109/JLT.2017.2781702, Journal of Lightwave Technology

Fig. 9 describes the repetition-rate and the pulse-duration variations as a function of the incident-pump-power for the Q-switched pulses from the proposed two sets of ring lasers operating in both C.W. and C.C.W. directions. Larger pump intensity leads to higher repetition rate and smaller pulse duration, which is a typical state of passively Q-switched scheme [64]. As for 0.9-m-length active fiber based Q-switched ring laser, in C.W. direction when the incident-pump-power was raised from 83.6 to 104.1 mW, the repetition-rate increased from 65.2 to 143.0 kHz, while in C.C.W. direction the Q-switched pulses experienced the variations of the repetition-rate boosting from 57.5 to 98.2 kHz, as shown in Fig. 9(a). One can see in Fig. 9(b), the corresponding pulse duration decreased from 3.9 to 1.35 μs in C.W. direction and from 1.92 to 0.81 μs in C.C.W. direction, respectively. Comparably, there is a similar feature shown in Fig. 9(c) and (d), illustrating the output characteristics of 1.4-m-length active fiber based Q-switched ring laser in both C.W. direction and C.C.W. direction. In C.W. direction, the output pulses have the repetition-rate range of 67.8-96.5 kHz and the pulse-duration range of 2.55-1.51 μs with the incident-pump-power increased from 86.7 to 102.3 mW. While in C.C.W. direction, the laser delivers the pulse trains with the repetition-rate range of 37.2-58.9 kHz and the pulse-duration range of 5.11-3.59 μs. These parameters embody the typical passively Q-switched features and are comparable to the previously-reported visible/infrared Q-switched all-fiber lasers enabled by other nanomaterial-based-SA [65]-[68]. Here, bidirectional red Q-switched output pulses with unsynchronized repetition rate from both C.W. and C.C.W. directions could be interpreted by the power-density difference acting on the SWNT-SA between two directions, which originates from the different-level gain and loss in both directions of the ring cavity.

For our experiments, under high intensity pumping, the SWNT-SA became over-saturation [18], which may be attributed to the performance of the fabricated SWNT-SA was not optimized for the red-light lasing wavelength [69]. Such a mechanism causes the pulse duration suddenly increased near the maximum incident pump power, as exhibited on the last 3 to 4 points of Fig. 9(b) and (d).

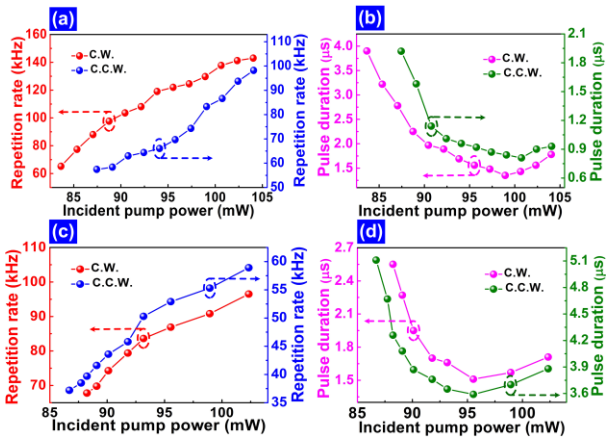

Fig. 9. Dependences of repetition rate and pulse duration on the incident pump power in both C.W. and C.C.W. operations, (a, b) for 0.9-m-length active fiber and (c, d) for 1.4-m-length active fiber, respectively.

Based on the above investigations, the output performances of two sets of bidirectional red Q-switched all-fiber ring lasers are summarized in Table I, which is meaningful to compare the Q-switching operations generated from different ring-cavity configurations. In Table I, one can clearly see that the output features are distinctive. The discrepancies, including the threshold incident-pump-power P_{th} and the maximum average-output-power P_{max} could be attributed to the changes of both the cavity design and intracavity polarization state. The reason that the PC was used to manage the outputs, is the random rotational orientation of the fibers in the ring resonator produces the polarization dependent loss [70]. The repetition-rate range (f_{rep}) is diversified with the incident-pump-power and exhibits a clear variation trend. The 0.9-m-length active fiber (i.e., L_{ac} = 0.9-m) based Q-switched ring laser shows better performance and the best one is from its C.W. direction: the repetition-rate range is about 80 kHz and the SNR reaches to ~43 dB. Moreover, such a laser exhibits shorter minimum pulse duration (τ_{min}) for both directions. And this experimental result is also consistent with the general prediction that the pulse duration is set by the cavity length in fiber lasers [71], namely, the pulse duration is shown to be directly proportional to the cavity round-trip time. In correspondence to the average-output-power P_{max}, the obtained maximum pulse energy (E_{max}) is also relatively low that is mainly determined by the laser ring cavity configuration.

TABLE I
OUTPUT COMPARISONS OF TWO SETS OF BIDIRECTIONAL RED-LIGHT PASSIVELY Q-SWITCHED ALL-FIBER RING LASERS WITH SWNT-SA

L_{ac}	Type	λ/nm	P_{th}/mW	P_{max}/mW	f_{rep}/kHz	τ_{min}/μs	E_{max}/nJ	SNR/dB
0.9-m	C.W.	635.4	83.6	0.39	65.2-143.0	1.35	2.73	43
	C.C.W.	635.4	87.1	0.29	57.5-98.2	0.81	2.95	40
1.4-m	C.W.	635.4	88.2	0.046	67.8-96.5	1.51	0.48	42
	C.C.W.	635.4	86.7	0.33	37.2-58.9	3.59	5.60	40

This article has been accepted for publication in a future issue of this journal, but has not been fully edited. Content may change prior to final publication. Citation information: DOI 10.1109/JLT.2017.2781702, Journal of Lightwave Technology

In our experiments, the mode-locking pulse was not achieved, and the reasons may be considered as follows: (1) the SWNT-SA for the red-light wavelength (i.e., 635 nm) was not optimal, including lower damage threshold and high nonsaturable loss, which are crucial for mode-locking pulse generation [72]-[75]. (2) The cavity design was not constructed for dispersion management [76]-[78]. Considering that it is a bit complicated in the case of our all-fiber-based laser cavity regime, which has non-negligible dispersion and $\chi(3)$ nonlinearity within the cavity, unlike in solid state laser cavities. The ongoing subject need to be accomplished for the visible mode-locking operation based on our ring cavity configuration with nanomaterial-based SAs, in that addressing the above-described challenges.

V. Conclusion

In summary, we experimentally demonstrate bidirectional red-light passively Q-switched all-fiber ring-cavity lasers incorporating a SWNT-based SA for the first time. Two sets of distinct output characteristics are performed by the combination of adjusting the cavity design and intra-cavity polarization state. The 0.9-m-length active fiber based Q-switched laser delivers the counter-circulating pulses with minimum pulse durations of 1.35 μs and 0.81 μs, respectively, the repetition rates ranging from 65.2 to 143 kHz and 57.5 to 98.2 kHz, respectively. As a comparison, the 1.4-m-length active fiber based Q-switched laser emits 1.51 μs and 3.59 μs minimum pulse durations, as well as the repetition rates of 37.2-96.5 kHz in both C.W. and C.C.W. directions. Such results not only further confirm the knowledge of ultra-broadband optical properties of SWNTs, but also provide a design guidance for the bidirectional Q-switched all-fiber ring lasers with selective outputs, which could find applications in sensing, medical and other versatile areas.

References

[1] V. Letokhov, "Laser biology and medicine," *Nature*, vol. 316, pp. 325-330, 1985.

[2] J. Limpert, F. Röser, S. Klingebiel, T. Schreiber, C. Wirth, T. Peschel, R. Eberhardt, and A. Tünnermann, "The rising power of fiber lasers and amplifiers," *IEEE J. Sel. Top. Quantum Electron.*, vol. 13, pp. 537-545, 2007.

[3] D. J. Richardson, J. Nilsson, W. A. Clarkson, "High power fiber lasers: current status and future perspectives," *J. Opt. Soc. Am. B*, vol. 27, pp. B63-B92, 2010.

[4] J. R. Taylor, "Tutorial on fiber-based sources for biophotonic applications," *J. Biomed. Opt.*, vol. 21, p. 061010, 2016.

[5] U. Keller, "Recent developments in compact ultrafast lasers," *Nature*, vol. 424, pp. 831-838, 2003.

[6] U. Keller, K. J. Weingarten, F. X. Kärtner, D. Kopf, B. Braun, I. D. Jung, R. Fluck, C. Hön ninger, N. Matuschek, and J. A. Der Au, "Semiconductor saturable absorber mirrors (SESAM's) for femtosecond to nanosecond pulse generation in solid-state lasers," *IEEE J. Sel. Top. Quantum Electron.*, vol. 2, pp. 435-453, 1996.

[7] O. Okhotnikov, A. Grudinin, and M. Pessa, "Ultra-fast fibre laser systems based on SESAM technology: New horizons and applications," *New J. Phys.*, vol. 6, p. 177, 2004.

[8] S. Y. Set, H. Yaguchi, Y. Tanaka, and M. Jablonski, "Ultrafast fiber pulsed lasers incorporating carbon nanotubes," *IEEE J. Sel. Top. Quantum Electron.*, vol. 10, pp. 137-146, 2004.

[9] Z. Sun, A. G. Rozhin, F. Wang, V. Scardaci, W. I. Milne, I. H. White, F. Hennrich, and A. C. Ferrari, "L-band ultrafast fiber laser mode locked by carbon nanotubes," *Appl. Phys. Lett.*, vol. 93, p. 061114, 2008.

[10] F. Wang, A. G. Rozhin, V. Scardaci, Z. Sun, F. Hennrich, I. H. White, W. I. Milne, and A. C. Ferrari, "Wideband-tuneable, nanotube mode-locked, fibre laser," *Nat. Nanotechnol.*, vol. 3, pp. 738-742, 2008.

[11] D. P. Zhou, L. Wei, B. Dong, and W. K. Liu, "Tunable passively Q-switched erbium-doped fiber laser with carbon nanotubes as a saturable absorber." *IEEE Photon. Technol. Lett.*, vol. 22, pp. 9-11, 2010.

[12] Q. Bao, H. Zhang, Y. Wang, Z. Ni, Y. Yan, Z. X. Shen, K. P. Loh, and D. Y. Tang, "Atomic-layer graphene as a saturable absorber for ultrafast pulsed lasers," *Adv. Funct. Mater.*, vol. 19, pp. 3077-3083, 2009.

[13] Z. Sun, T. Hasan, F. Torrisi, D. Popa, G. Privitera, F. Wang, F. Bonaccorso, D. M. Basko, and A. C. Ferrari, "Graphene mode-locked ultrafast laser," *ACS nano*, vol. 4, pp. 803-810, 2010.

[14] Z. Luo, M. Zhou, J. Weng, G. Huang, H. Xu, C. Ye, and Z. Cai, "Graphene-based passively Q-switched dual-wavelength erbium-doped fiber laser," *Opt. Lett.*, vol. 35, pp. 3709-3711, 2010.

[15] A. Martinez and Z. Sun, "Nanotube and graphene saturable absorbers for fibre lasers," *Nat. Photon.*, vol. 7, pp. 842-845, 2013.

[16] C. Wei, X. Zhu, F. Wang, Y. Xu, K. Balakrishnan, F. Song, R. A. Norwood, and N. Peyghambarian, "Graphene Q-switched 2.78 μm Er^{3+}-doped fluoride fiber laser," *Opt. Lett.*, vol. 38, pp. 3233-3236, 2013.

[17] H. Zhang, S. Lu, J. Zheng, J. Du, S. Wen, D. Tang, and K. Loh, "Molybdenum disulfide (MoS_2) as a broadband saturable absorber for ultra-fast photonics," *Opt. Express*, vol. 22, pp. 7249-7260, 2014.

[18] Z. Luo, Y. Huang, M. Zhong, Y. Li, J. Wu, B. Xu, H. Xu, Z. Cai, J. Peng, and J. Weng, "1-, 1.5-, and 2-μm fiber lasers Q-switched by a broadband few-layer MoS_2 saturable absorber," *J. Lightwave Technol.*, vol. 32, pp. 4077-4084, 2014.

[19] K. Wu, X. Zhang, J. Wang, X. Li, and J. Chen, "WS_2 as a saturable absorber for ultrafast photonic applications of mode-locked and Q-switched lasers," *Opt. Express*, vol. 23, pp. 11453-11461, 2015.

[20] M. Jung, J. Lee, J. Park, J. Koo, Y. M. Jhon, and J. H. Lee, "Mode-locked, 1.94-μm, all-fiberized laser using WS_2-based evanescent field interaction," *Opt. Express*, vol. 23, pp. 19996-20006, 2015.

[21] R. I. Woodward, R. C. T. Howe, G. Hu, F. Torrisi, M. Zhang, T. Hasan, and E. J. R. Kelleher, "Few-layer MoS_2 saturable absorbers for short-pulse laser technology: current status and future perspectives," *Photonics Res.*, vol. 3, pp. A30-A42, 2015.

[22] J. Koo, Y. I. Jhon, J. Park, J. Lee, Y. M. Jhon, and J. H. Lee, "Near-infrared saturable absorption of defective bulk-structured WTe_2 for femtosecond laser mode-locking," *Adv. Funct. Mater.*, vol. 26, pp. 7454-7461, 2016.

[23] D. Mao, B. Du, D. Yang, S. Zhang, Y. Wang, W. Zhang, X. She, H. Cheng, H. Zeng, and J. Zhao, "Nonlinear saturable absorption of liquid-exfoliated molybdenum/tungsten ditelluride nanosheets," *Small*, vol. 12, pp. 1489-1497, 2016.

[24] C. Zhao, H. Zhang, X. Qi, Y. Chen, Z. Wang, S. Wen, and D. Tang, "Ultra-short pulse generation by a topological insulator based saturable absorber," *Appl. Phys. Lett.*, vol. 101, p. 211106, 2012.

[25] Z. -C. Luo, M. Liu, H. Liu, X. -W. Zheng, A. -P. Luo, Zheng, A. -P. Luo, C. -J. Zhao, H. Zhang, S. -C. Wen, and W. -C. Xu, "2 GHz passively harmonic mode locked fiber laser by a microfiber-based topological insulator saturable absorber," *Opt. Lett.*, vol. 38, pp. 5212-5215, 2013.

[26] Z. Luo, C. Liu, Y. Huang, D. Wu, J. Wu, H. Xu, Z. Cai, Z. Lin, L. Sun, and J. Weng, "Topological-insulator passively Q-switched double-clad fiber laser at 2 μm wavelength," *IEEE J. Sel. Top. Quantum Electron.*, vol. 20, p. 0902708, 2014.

[27] J. Boguslawski, J. Sotor, G. Sobon, J. Tarka, J. Jagiello, W. Macherzynski, L. Lipinska, and K. M. Abramski, "Mode-locked Er-doped fiber laser based on liquid phase exfoliated Sb_2Te_3 topological insulator," *Laser Phys.*, vol. 24, p. 105111, 2014.

[28] M. Jung, J. Lee, J. Koo, J. Park, Y. W. Song, K. Lee, S. Lee, and J. H. Lee, "A femtosecond pulse fiber laser at 1935 nm using a bulk-structured Bi_2Te_3 topological insulator," *Opt. Express*, vol. 22, pp. 7865-7874, 2014.

[29] J. Lee, J. Koo, Y. -M. Jhon, and J. H. Lee, "A femtosecond pulse erbium fiber laser incorporating a saturable absorber based on a bulk-structured Bi_2Te_3 topological insulator," *Opt. Express*, vol. 22, pp. 6165-6173, 2014.

[30] J. Lee, M. Jung, J. Koo, C. Chi, and J. H. Lee, "Passively Q-switched 1.89-μm fiber laser using a bulk-structured Bi_2Te_3 topological insulator," *IEEE J. Sel. Top. Quantum Electron.*, vol. 21, p. 0900206, 2015.

[31] H. Mu, S. Lin, Z. Wang, S. Xiao, P. Li, Y. Chen, H. Zhang, H. Bao, S. Lau, C. Pan, D. Fan, and Q. Bao "Black phosphorus-polymer composites for pulsed lasers," *Adv. Opt. Mater.*, vol. 3, pp. 1447-1453, 2015.

[32] Y. Chen, G. Jiang, S. Chen, Z. Guo, X. Yu, C. Zhao, H. Zhang, Q. Bao, S. Wen, D. Tang, and D. Fan, "Mechanically exfoliated black phosphorus as a new saturable absorber for both Q-switching and mode-locking laser operation," *Opt. Express*, vol. 23, pp. 12823-12833, 2015.

[33] J. Sotor, G. Sobon, M. Kowalczyk, W. Macherzynski, P. Paletko, and K. M. Abramski, "Ultrafast thulium-doped fiber laser mode locked with black phosphorus," *Opt. Lett.*, vol. 40, pp. 3885-3888, 2015.

[34] Z. -C. Luo, M. Liu, Z. -N. Guo, X. -F. Jiang, A. -P. Luo, C. -J. Zhao, X. -F. Yu, W. -C. Xu, and H. Zhang, "Microfiber-based few-layer black phosphorus saturable absorber for ultra-fast fiber laser," *Opt. Express*, vol. 23, pp. 20030-20039, 2015.
[35] S. B. Lu, L. L. Miao, Z. N. Guo, X. Qi, C. J. Zhao, H. Zhang, S. C. Wen, D. Y. Tang, and D. Y. Fan, "Broadband nonlinear optical response in multi-layer black phosphorus: an emerging infrared and mid-infrared optical material," *Opt. Express*, vol. 23, pp. 11183-11194, 2015.
[36] J. Lee, B. -K. Yu, Y. I. Jhon, J. Koo, S. J. Kim, Y. M. Jhon, and J. H. Lee, "Filled skutterudites for broadband saturable absorbers," *Adv. Opt. Mater.*, vol. 5, p. 1700096, 2017.
[37] Y. I. Jhon, J. Koo, B. Anasori, M. Seo, J. H. Lee, Y. Gogotsi, and Y. M. Jhon, "Metallic MXene saturable absorber for femtosecond mode-locked lasers," *Adv. Mater.*, vol. 29, p. 1702496, 2017.
[38] Z. Luo, D. Wu, B. Xu, H. Xu, Z. Cai, J. Peng, J. Weng, S. Xu, C. Zhu, F. Wang, and Z. Sun "Two-dimensional material-based saturable absorbers: Towards compact visible-wavelength all-fiber pulsed lasers," *Nanoscale*, vol. 8, pp. 1066-1072, 2016.
[39] W. Li, J. Peng, Y. Zhong, D. Wu, H. Lin, Y. Cheng, Z. Luo, J. Weng, H. Xu, and Z. Cai, "Orange-light passively Q-switched Pr^{3+}-doped all-fiber lasers with transition-metal dichalcogenide saturable absorbers," *Opt. Mater. Express*, vol. 6, pp. 2031-2039, 2016.
[40] D. Wu, Z. Cai, Y. Zhong, J. Peng, J. Weng, Z. Luo, N. Chen, and H. Xu, "635 nm visible Pr^{3+}-doped ZBLAN fiber lasers Q-switched by topological insulators SAs," *IEEE Photon. Technol. Lett.*, vol. 27, pp.2379-2382, 2015.
[41] D. Wu, Z. Cai, Y. Zhong, J. Peng, Y. Cheng, J. Weng, Z. Luo, and H. Xu, "Compact passive Q-switching Pr^{3+}-doped ZBLAN fiber laser with black phosphorus-based saturable absorber," *IEEE J. Sel. Top. Quantum Electron.*, vol. 23, p. 0900106, 2017.
[42] J. S. Lauret, C. Voisin, G. Cassabois, C. Delalande, Ph. Roussignol, O. Jost, and L. Capes, "Ultrafast carrier dynamics in single-wall carbon nanotubes," *Phys. Rev. Lett.*, vol. 90, p. 057404, 2003.
[43] S. Yamashita, Y. Inoue, S. Maruyama, Y. Murakami, H. Yaguchi, M. Jablonski, and S. Set, "Saturable absorbers incorporating carbon nanotubes directly synthesized onto substrates and fibers and their application to mode-locked fiber lasers," *Opt. Lett.*, vol. 29, pp. 1581-1583, 2004.
[44] T. Hasan, Z. Sun, F. Wang, F. Bonaccorso, P. H. Tan, A. G. Rozhin, and A. C. Ferrari, "Nanotube-polymer composites for ultrafast photonics," *Adv. Mater.*, vol. 21, pp. 3874-3899, 2009.
[45] F. Wang, A. G. Rozhin, Z. Sun, V. Scardaci, R. V. Penty, I. H. White, and A. C. Ferrari, "Fabrication, characterization and mode locking application of single-walled carbon nanotube/polymer composite saturable absorbers," *Int. J. Mater. Form.*, vol. 1, pp. 107-112, 2008.
[46] E. J. R. Kelleher, J. C. Travers, Z. Sun, A. G. Rozhin, A. C. Ferrari, S. V. Popov, and J. R. Taylor, "Nanosecond-pulse fiber lasers mode-locked with nanotubes," *Appl. Phys. Lett.*, vol. 95, p. 111108, 2009.
[47] B. Dong, C. Liaw, J. Hao, and J. Hu, "Nanotube Q-switched low-threshold linear cavity tunable erbium-doped fiber laser," *Appl. Opt.*, vol. 49, pp. 5989-5992, 2010.
[48] M. Jung, J. Koo, Y. M. Chang, P. Debnath, Y. -W. Song, and J. H. Lee, "An all fiberized, 1.89-μm Q-switched laser employing carbon nanotube evanescent field interaction", *Laser. Phys. Lett.*, Vol. 9, pp. 669-673, 2014.
[49] Y. Meng, Y. Li, Y. Xu, and F. Wang, "Carbon Nanotube Mode-Locked Thulium Fiber Laser With 200 nm Tuning Range," *Sci. Rep.*, vol. 7, p. 45109, 2017.
[50] S. Xu, F. Wang, C. Zhu, Y. Meng, Y. Liu, W. Liu, J. Tang, K. Liu, G. Hu, R. C. T. Howe, T. Hasan, R. Zhang, Y. Shi, and Y. Xu, "Ultrafast nonlinear photoresponse of single-wall carbon nanotubes: a broadband degenerate investigation," *Nanoscale*, vol. 8, pp. 9304-9309, 2016.
[51] W. Li, T. Du, J. Lan, C. Guo, Y. Cheng, H. Xu, C. Zhu, F. Wang, Z. Luo, and Z. Cai, "716 nm deep-red passively Q-switched Pr:ZBLAN all-fiber laser using a carbon-nanotube saturable absorber," *Opt. Lett.*, vol. 42, pp. 671-674, 2017.
[52] F. Aronowitz, "Theory of a traveling wave optical maser," *Phys. Rev.*, vol. 139, pp. A635-A646, 1965.
[53] H. Zeghlache, P. Mandel, N. B. Abraham, L. M. Hoffer, G. L. Lippi, T. Mello, "Bidirectional ring laser: Stability analysis and time-dependent solutions," *Phys. Rev. A*, vol. 37, pp. 470-497, 1988.
[54] N. D. Lai, F. Bretenaker, and M. Brunel, "Coherence of pulsed microwave signals carried by two-frequency solid state lasers," *J. Lightwave Technol.*, vol. 21, pp. 3037-3042, 2003.
[55] M. Brunel, M. Vallet, "Pulse-to-pulse coherent beat note generated by a passively Q-switched two-frequency laser," *Opt. Lett.*, vol. 33, pp. 2524-2526, 2008.
[56] C. Ouyang, P. Shum, K. Wu, J. H. Wong, H. Q. Lam, and S. Aditya, "Bidirectional passively mode-locked soliton fiber laser with a four-port circulator," *Opt. Lett.*, vol. 36, pp. 2089-2091, 2011.
[57] K. Kieu and M. Mansuripur, "All-fiber birectional passively mode-locked ring laser," *Opt. Lett.*, vol. 33, pp. 64-66, 2008.
[58] S. Lu, C. Zhao, Y. Zou, S. Chen, Y. Chen, Y. Li, H. Zhang, S. Wen, and D. Tang, "Third order nonlinear optical property of Bi_2Se_3," *Opt. Express*, vol. 21, pp. 2072-2082, 2013.
[59] G. P. Agrawal, Applications of Nonlinear Fiber Optics, Academic Press, San Diego, 2001.
[60] H. H. Liu, and K. K. Chow, "Operation-switchable bidirectional pulsed fiber laser incorporating carbon-nanotube-based saturable absorber," *IEEE J. Sel. Top. Quantum Electron.*, vol. 20, p. 0901905, 2014.
[61] Y. Chen, C. Zhao, H. Huang, S. Chen, P. Tang, Z. Wang, S. Lu, H. Zhang, S. Wen, and D. Tang, "Self-assembled topological insulator: Bi_2Se_3 membrane as a passive Q-switcher in an erbium-doped fiber laser," *J. Lightwave Technol.*, vol. 31, pp. 2857-2863, 2013.
[62] R. I. Woodward and E. J. R. Kelleher, "2D saturable absorbers for fibre lasers," *Appl. Sci.*, vol. 5, pp. 1440-1456, 2015.
[63] Z. Sun, A. Martinez, and F. Wang, "Optical modulators with two dimensional layered materials," *Nat. Photon.*, vol. 10, pp. 227-238, 2016.
[64] J. Li, H. Luo, B. Zhai, R. Lu, Z. Guo, H. Zhang, and Y. Lu, "Black phosphorus: a two-dimension saturable absorption material for mid-infrared Q-switched and mode-locked fiber lasers," *Sci. Rep.*, vol. 6, p. 30361, 2016.
[65] D. Popa, Z. Sun, T. Hasan, F. Torrisi, F. Wang, and A. C. Ferrari, "Graphene Q-switched, tunable fiber laser," *Appl. Phys. Lett.*, vol. 98, p. 073106, 2011.
[66] Y. Chen, C. Zhao, S. Chen, J. Du, P. Tang, G. Jiang, H. Zhang, S. Wen, and D. Tang, "Large energy, wavelength widely tunable, topological insulator Q-switched erbium-doped fiber laser," *IEEE J. Sel. Top. Quantum Electron.*, vol. 20, p. 0900508, 2014.
[67] X. Li, Y. Wang, Y. Wang, W. Zhao, X. Yu, Z. Sun, X. Cheng, X. Yu, Y. Zhang, and Q. Wang, "Nonlinear absorption of SWNT film and its effects to the operation state of pulsed fiber laser," *Opt. Express*, vol. 22, pp. 17227-17235, 2014.
[68] M. Zhang, G. Hu, G. Hu, R. C. T. Howe, L. Chen, Z. Zheng, and T. Hasan, "Yb- and Er-doped fiber laser Q-switched with an optically uniform, broadband WS_2 saturable absorber," *Sci. Rep.*, vol. 5, p. 17482, 2015.
[69] F. Wang, S. Xu, H. Hong, R. Howe, K. Liu, T. Hasan, and Y. Xu, "Ultrafast nonlinear absorption in SWNTs: an ultra-broadband investigation," in *IEEE CLEO-PR*, Busan, Korea, 2015, vol. 1, pp. 1-2.
[70] R. Al-Mahrous, R. Caspary, and W. Kowalsky, "Red fiber ring lasers," in *IEEE ICTON*, Azores, Portugal, 2009, pp. 1-5.
[71] R. Herda, S. Kivistö, and O. G. Okhotnikov, "Dynamic gain induced pulse shortening in Q-switched lasers," *Opt, Lett.*, vol. 33, pp. 1011-1013, 2008.
[72] Y. W. Song, S. Yamashita, and S. Maruyama, "Single-walled carbon nanotubes for high-energy optical pulse formation," *Appl. Phys. Lett.*, vol. 92, p. 021115, 2008.
[73] Z. Sun, A. G. Rozhin, F. Wang, T. Hasan, D. Popa, W. O'Neill, and A. C. Ferrari, "A compact, high power, ultrafast laser mode-locked by carbon nanotubes," *Appl. Phys. Lett.*, vol. 95, p. 253102, 2009.
[74] P. Yan, A. Liu, Y. Chen, H. Chen, S. Ruan, C. Guo, S. Chen, I. L. Li, H. Yang, and J. Hu, "Microfiber -based WS_2-film saturable absorber for ultrafast photonics," *Opt. Mater. Express*, vol. 5, pp. 479-489, 2015.
[75] X. Liu, Q. Guo, and J. Qiu, "Emerging low-dimensional materials for nonlinear optics and ultrafast photonics," *Adv. Mater.*, vol. 29, p. 1605886, 2017.
[76] Z. Sun, T. Hasan, F. Wang, A. G. Rozhin, I. H. White, and A. C. Ferrari, "Ultrafast stretched-pulse fiber laser mode-locked by carbon nanotubes," *Nano Research*, vol. 3, pp. 404-411, 2010.
[77] J. Jeon, J. Lee, and J. H. Lee, "Numerical study on the minimum modulation depth of a saturable absorber for stable fiber laser mode locking," *J. Opt. Soc. Am. B*, vol. 32, pp. 31-37, 2015.
[78] D. Mao, Y. Wang, C. Ma, L. Han, B. Jiang, X. Gan, S. Hua, W. Zhang, T. Mei, and J. Zhao, "WS_2 mode-locked ultrafast fiber laser," *Sci. Rep.*, vol. 5, p. 7965, 2015.